doi.org/10.36721/PJPS.2022.35.4.SP.1181-1190.1

Design, synthesis, ADME, biological evaluation and molecular dynamic studies of natural and synthetic remedy of *Herpes simplex* virus type-1

Suhad Sami Humadi[1], Samir Mohamed Awad[2], Ahmed Abd Elkader El-Rashedy[3] and Mohamed Fathy El-Shehry[4*]

[1]Al-Zahrawi University College, Department of Pharmacy, Karbala, Iraq
[2]Pharmaceutical Organic Chemistry Department, Faculty of Pharmacy, Helwan University, Egypt
[3]Department of Natural and Microbial Product, National Research Centre, Dokki, Cairo, Egypt
[4]Department of Pesticide Chemistry, National Research Centre, Dokki, Egypt

Abstract: Garlic (known as; *Allium sativum*) is one of the most widely used medicinal plants in the world. Allicin is the major agent of garlic that gives its known pharmacological activities as anti-inflammatory, antibacterial, antifungal, antiviral and antioxidant agent. It could be extracted from bulbs of *Allium sativum* by water extraction to give allicin in low yield therefore other better methods were followed for extraction such as ultrasonic-assisted method that gives good yield. Attempts to optimize allicin extraction were found with sliced garlic at 25 °C for 90 minute of extraction for maximum yield (112µg/mL). Allicin was subjected to its evaluation as anti-herpetic against herpes simplex virus 1 (HSV-1) and exhibited a promising activity compared to acyclovir which was used as a reference standard. On the other hand, a novel synthetic amantadine derivative was evaluated as antiherpetic agent and prepared from the reaction of 2-thiouracil-5-sulphonyl chloride with amantadine hydrochloride in pyridine. The synergestic effect of allicin and the amantadine derivative was evaluated against HSV-1, using both in silico molecular docking as for dynamics simulations. Thymidine kinase target enzyme was chosen to analyze any possible interactions, as well as any protein-ligand stability. Furthermore, some of properties of the potential HSV-1 thymidine kinase target inhibitor of the amantadine derivative were analyzed.

Keywords: Antiviral, allicin and amantadine derivative as antiherpetic agents, molecular modeling, molecular dynamic, ADME.

INTRODUCTION

No voice is louder than the war on viruses, that deadly enemy. Rather, we can say that is the third world war and urgent need that everyone is rushing to provide the most powerful antiviral agents, but they are few and most of them are not effective in the required form. Therefore, natural products were resorted to and their effectiveness was adopted. Now, garlic is an example of phytomedicinals recommended by herbalists and doctors for the prophylaxis, treatment of various diseases and as herb protector in medicine medicine (Yoshiteru *et al*., 2006; Holsinger *et al*., 1994; Bright *et al*., 2000; Zandi *et al*., 2009; Alen *et al*., 2011; Hadi *et al*., 2019). Allicin is the principle thiosulfinates content of this important plant extract (Harazem *et al*., 2019). It is flowed when garlic cloves are crushed, cut, or chewed. The *S*-(+)-allyl-*L*-cyteinesulfoxide (Allin) inside the cells quickly breaks into allicin and other sulphur containing compounds under the effect of allinase as a hydrolytic enzyme. Biologically, allicin is an effective antibacterial and antiviral agent, in addition to its antioxidant activity (Rahman *et al*., 2011). Variable methods were used to attain high yield ratio from its extraction from garlic. For example, a common method is using pressurized liquid extraction technique with ethanol as the solved, also by using reversed-phase HPLC method to analyze allicin in garlic extracts (Vioreca *et al*., 2021). In addition, an advanced method is the ultrasonic-assisted extraction technique that gives high yield of allicin which was used in our research (Ranitha *et al*., 2017). Furthermore, amantadine is well-identified as antiviral agent; it was first used for treatment of influenza (Hubsher *et al*., 2012) and its antiviral activity was reported during 1963. Currently, it is no longer recommended for the treatment of influenza since early 2000s (Balgi *et al*., 2013). Here in our work, we incorporate amantadine with 2-thiouracil to investigate the antiviral activity of the produced derivative as anti-herpetic agent.

MATERIALS AND METHODS

Plant Samples

Garlic cloves were bought from an Egyptian market which was originated from El-Minya governorate-Egypt; all samples were identified and preserved in laboratory at suitable circumstances (dark, 16^{o}C) in a dry well ventilated lab in addition to being cool.

**Corresponding author:* e-mail: mohamedelshehry2000@gmail.com

Reagents

99.9% Methanol (Highly purified) imported from Sigma Aldrich (US). De-ionized water samples were handled and refined by; Milli-Q purification system (Millipore) (Massachusetts, USA).

Pretreatments

A mixture of 10g of garlic cloves with 100 mL distilled H_2O were homogenized for 1 minute in a commercial blender. The Sliced sample composed of; 10g of sliced garlic cloves with an equal size mixed with ≈100ml distilled H_2O.

Ultrasonic-Assisted Extraction (UAE)

UAE was carried out, at standardized conditions, in an ultrasound cleaning bath (Sonorex DT1034/H, 500mm x 300 mm x 200 mm interior dimensions) by using indirect sonication method, using the fixed-frequency of 35 KHV as the working liquid. The pre-heated sample mixture was treated for the extraction process, through charged in 100 ml sample flask and admitted into the ultrasonic cavity. Some conditions were adopted in such a way that, extraction time was attained (every 30 min till 150min.), extraction temperature (25°C, 30°C, 35°C) and particle size of both blended and/or sliced garlic bulb. Centrifugation of the solution at 3,000g for 2min was performed after sonication, then filtration from impurities and the remaining undissolved garlic and stored at 4°C.

Quantification of Allicin

Quantification process of Allicin in garlic extract was performed using HPLC method, as reported in by Ranitha Mathialagan (Liu *et al*., 2010).

Molecular Docking and Dynamics Studies

Based on the *in vitro* antiviral assays, our target amantadine derivative was further subjected for computational studies to investigate its mode of action at the molecular level. Molecular docking studies were performed on the viral thymidine kinases of HSV-1 to predicate the binding affinity and the interaction of the amantadine derivative toward the HSV-1 thymidine kinase receptor, which was chosen based on the pharm mapper server screening (Liu *et al*., 2010). A preliminary molecular docking simulation was performed to assess the putative binding mode of the compound with the proposed targets. Finally, the inhibitory mechanism were revealedusing molecular dynamic, accompanied with the selectivity and specificity of these target inhibitors toward main receptors.

Molecular dynamic methods

System preparation

The thymidine kinase X-ray crystal structures, an effective enzyme in HSV-1 and its complex penciclovir was repossessed from the protein data bank, following the reported methods in literature (Champness *et al*., 1998; Pettersen *et al*., 2004; Li *et al*., 2005).

Molecular dynamic (MD) simulations

Recently, MD simulations became one of main techniques used to investigate some kinetics of different particles and molecules that would otherwise hardly detected in biological system (Hospital *et al*., 2015). Providinga detailed information on the dynamical progression of molecular interaction and conformational changes, in biological systems. The GPU version of the PMEMD engine included in the AMBER 18 platform was used to run MD simulations of all modes (Lee *et al*., 2018). The compound's partial atomic charge was calculated utilizing ANTECHAMBER general amber force field (GAFF) methodology, as revealed in literature (Wang *et al*., 2006; Roe *et al*., 2013). [See; supplementary date for full methods]

Post-MD Analysis

The origin (Seifert *et al*., 2014) data analysis program and Chimera (Pettersen *et al*., 2004) were used to create all graphs and visualizationsm as reported in literature (Genheden *et al*., 2015; Kollman *et al*., 2000; Drissi *et al*., 2015; Hayes *et al*., 2012).

Thermodynamic calculation

Binding free energy was calculated by averaging 500 photos from the full 50ns trajectory. The following is a representation of the difference in linking free energy (G) for each molecular species (complex, ligand and receptor), (fig. 1): (Genheden *et al*., 2015; Hou *et al*., 2010):

$$\Delta G_{bind} = G_{complex} - G_{receptor} - G_{ligand} \quad (1)$$

$$\Delta G_{bind} = E_{gas} + G_{sol} - TS \quad (2)$$

$$E_{gas} = E_{int} + E_{vdw} + E_{ele} \quad (3)$$

$$G_{sol} = G_{GB} + G_{SA} \quad (4)$$

$$G_{SA} = \gamma SASA \quad (5)$$

Egas (gas-phase energy) — Eint (internal energy)

Eele (Coulomb energy) — Evdw (van der Waals energy)

S (solute's total entropy) — T(temperature)

Note: Each residue contributes to the total binding free energy obtained at the predicated active site by carrying out per-Residue energy decomposition at the atomic level using the MM/GBSA method in AMBER 18.

Fig. 1: Thermodynamic calculation

The Egas was calculated the FF14SB force field terms directly. The solvation free energy (Gsol) (G) were calculates from: (GGB) the polar states and non-polar states (Gsol)

The non-polar solvation free energy (Gsol) was calculates from: Solvent Accessible Surface Area (SASA), using a water probe radius of 1.4. The polar solvation (GGB) contribution was evaluated by solving the GB equation.

ADME prediction

Swiss ADME, (http://www.swissadme.ch/), was used to analyze different physico-chemical properties, in addition to the pharmacokinetic and pharmaco dynamic characteristics. OSIRIS property was used to calculate the toxicity parameters such as mutagenicity, tumorigenicity, irritating effects and reproductive effects.

Chemistry

Experimental

The commercial used reagents and solvents were not purified. The purity of all compounds and follow up the reactions progress were checked with GC and TLC. Silica gel-precoated TLC chromatography aluminum sheets (Type 60 F254, Merck); UV (254nm) or iodine were used to locate the spots.Gallenkamp-5 apparatus measure all melting points (uncorr.) in open capillary tubes. ^{1}HNMR,on Jeol 500MHz spectrometer and^{13}CNMR, on Bruker 125 MHz NMR spectrometer spectra were performed in DMSO-d_6 (^{1}H) and (^{13}C) instruments, chemical shifts (δ) were stated in ppm. Mass spectra were determined applying the electron impact technique (EI), by a MAT Finnigan SSQ 7000 spectrometer.

Synthesis of 4-oxo-2-thioxo-1,2,3,4-tetrahydropyrimidine-5-sulphonic acid-N-adamantyl amide

A mixture of 2-thiouracil-5-sulfonyl chloride (1.13g, 0.005mol) and amantadine HCl (1.01g, 0.005mol) in 25ml pyridine was heated using reflux apparatus for about 8h. The resultant mixture was then chilled, using crushed ice and counter balanced with HCl (dil.), the produced solid was filtered off, washed numerous times with H_2O then via pet. Ether, dried & crystallized from DMF/ water.

Eluent: hexane/EAA (94/6, v/v). *N*-adamantyl amide was separated as; yellow crystals of yield 85%. mp 281-283 ^{o}C. IR (KBr) (ῡmax,cm-1): 3425, 3319, 3178 (3NH`s), 1749 (C=O), 1586 (C=C), 1300 (C=S) cm$^{-1}$; $^{1}$H NMR (500.1 MHz, DMSO-$d^6$): δ 1.85-1.09 (m, 15H); 2.31 (s, 2H-$CH_2$); 8.14 (s, 1$H_{pyr}$), 9.61, 10.51, 11.18 (3s, 3H, 3 NH`s). ^{13}C NMR (125 MHz, DMSO-d^6): 25.93 (3C_3-Ada); 30.66 (C_4-Ada); 34.81 (C_2-Ada); 40.75 (CH_2); 56.93 (3C_2-Ada); 119.07 (C-5$_{pyr}$); 149.07 (C-6$_{pyr}$); 167.91(CO), 178.48 (CS). MS (EI 70 eV): m/z (%) = 340 (15) [M^+]. Anal. Calcd for $C_{14}H_{19}N_3O_3S_2$ (341.45): C, 49.25; H, 5.61; N, 12.31. Found: C, 49.59; H, 5.30; N, 12.41.

Biology method (K.Zandi et al) (Saif *et al*., 2020; Samir *et al*., 2021)

Cell and virus

Vero cell line; from African green monkey kidney cell line, was uploaded as an appropriate cell line for HSV-1 propagation. The cells were cultured using Dulbeco minimum (Gibco) provided with 10% fetal bovine serum (Gibco). The antiviral screening was conducted on the KOS strain of HSV-1. Applying Vero cells for the virus propagated, the titer of propagated viral stock was firmed, using Karber's method, as $TCID_{50}$ mL^{-1}. After titration viral stock was stored at -70^{o}C until whenever used in sterile tubes.

Synthesis of examined compounds and the standard

Acyclovir, from Sigma, amantadine derivative and allicin were adopted as mentioned earlier. Dimethyl sulfoxide (DMSO) was employed as a proper diluent for analyzed compounds and acyclovir.

Determination of antiviral assay

The cytopathic inhibition assay (Saif *et al*., 2020) was adopted as a first choice to ascertain the semi-quantitative antiviral property of each analyzed compound, following the full methods described in supplementary data. The Results of the inhibition of HSV-1 related cytopathic effect (CPE) by utilizing various strengths of examined compounds and standard. Each value is the average of four replicate analyses; summarized (table 1 & fig. 2)

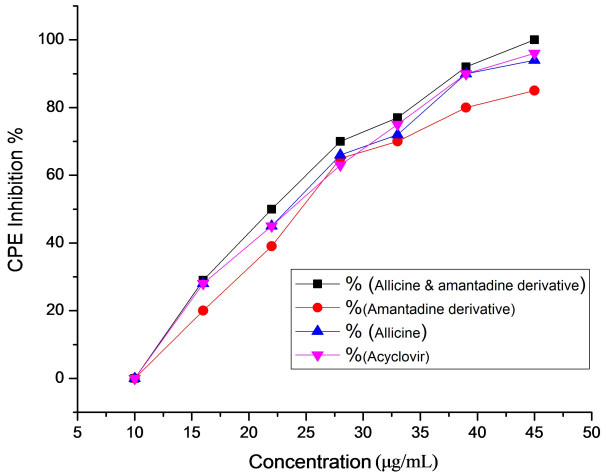

Fig. 2: The antiviral activity of active mixture of Allicin & the amantadine sulfonamide derivative was investigated at different concentrations (µg/mL).

RESULTS

Chemistry

Huge numbers of antiviral medicines are prescribed for curing herpes as acyclovir, valacyclovir, famicyclovir and pencyclovir (fig. 3). Acyclovir was the earliest proposed candidate and is now presented in generic forms. Valcyclovir is also offered as a generic item and is slightly more efficient over acyclovir for decreasing lesion recovery time. Infections by HSV-1 are grouped depending on the position of the body diseased. It could give rise to cold sores which are collections of tiny boils, as well as leading to a sore throat. Based on these findings, our strategy to concentrate on a natural product extracted from garlic and synthesize of amantadine sulfonamide derivative from reaction of 2-thiouracil-5-sulfonyl chloride with amantadine hydrochloride in dry

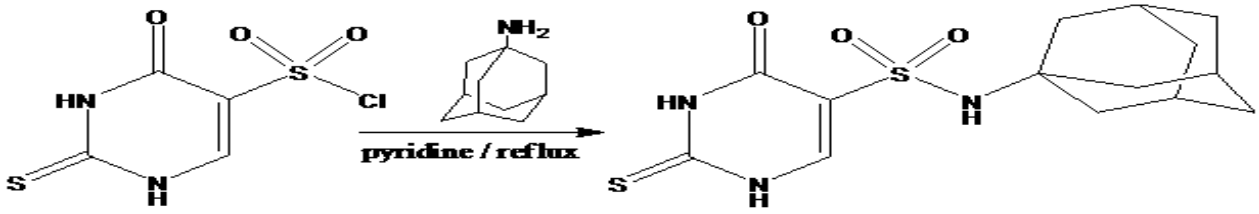

Scheme 1: Structure of 5-adamantyl-2-thiopyrimidine sulphonamide.

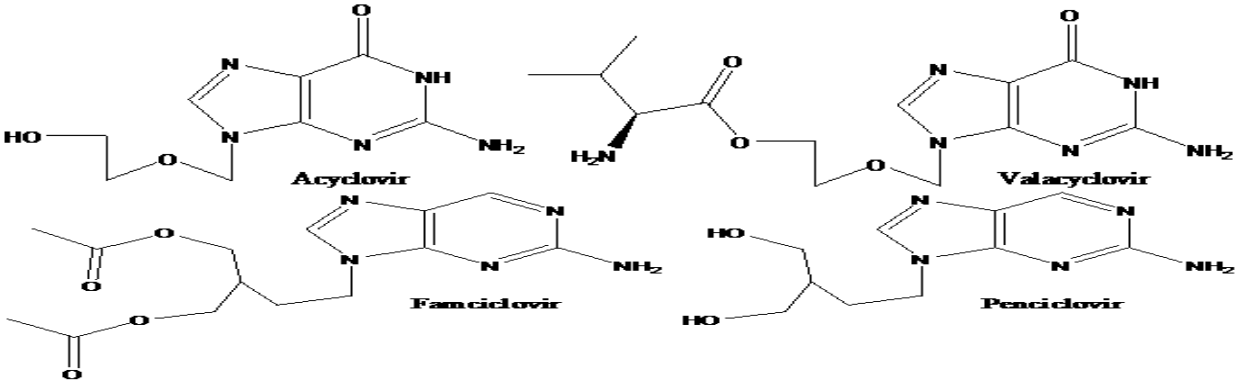

Fig. 3: Antiviral drugs structures.

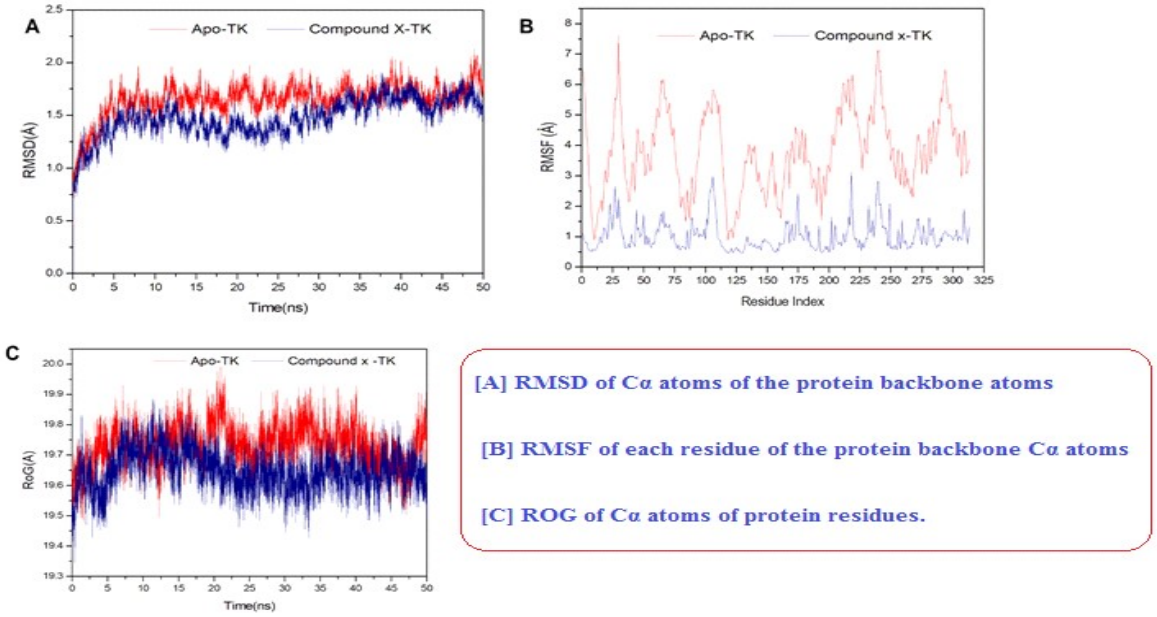

Fig. 4: Molecular dynamic and system stability representation.

pyridine as a solvent as an acid binder yielding the corresponding expected product in good yield (Scheme 1).

Molecular dynamic and system stability

MD simulations were carried out to show the inhibition action and interactions of the potential ligand and HSV-1 thymidine kinase target (TK). System stability validation is a major tool in tracing unsettled movements and avoid artifacts that may appear during the simulation. In our research, Root-Mean-Square Deviation (RMSD) was computed to measure the systems' stability throughout the 50 ns simulations (fig. 4A). The documented median RMSD amounts for all settings of systems Apo-TK and amantadine sulfonamide derivative-TK were 1.65Å and 1.47Å, in that order.

Mechanism of binding interactions based on binding free energy calculation

Drug-ligand binding data provides a valuable means in the structural basis for that ligand's activity. Consequently, calculating protein-ligand binding affinities depending on free binding free energy computations is a crucial method to uncover new protein inhibitors (Cournia *et al*., 2017) (table 2),

Table 1: The inhibition of HSV-1 related cytopathic effect (CPE)

Dose (µg/mL)	CPE inhibition			
	Acyclovir	Allicin	Amantadine derivative	Allicin& Amantadine derivative
10	0	0	0	0
16	29±2	20±1	28±1	28±1
22	50±1	39±1	45±1	45±1
28	70±2	65±1	66±8	63±2
33	77±3	70±1	72±2	75±2
39	92±1	80±2	90±2	90±1
45	98±2	85±2	94±2	96±2

Data presented as mean ± SD, n=3. Statistical analysis is carried out using Co-state and SPSS computer programs (version 7), where unshared letter is significant at P≤0.05.

Table 2: The energy binding calculated for the *N*-amantadine derivative against HSV-1(TK)

Energy Components (kcal/mol)					
Complex	ΔE_{vdW}	ΔE_{elec}	ΔG_{gas}	ΔG_{solv}	ΔG_{bind}
amantadine derivative	-43.85± 0.31	--34.37±0.89	-78.22± 0.91	37.46±0.81	-40.75± 0.54
ΔE_{vdW} = van der Waals energyΔ_{Eele} = electrostatic energy ΔG_{solv} = solvation free energyΔG_{bind} = calculated total binding free energy					

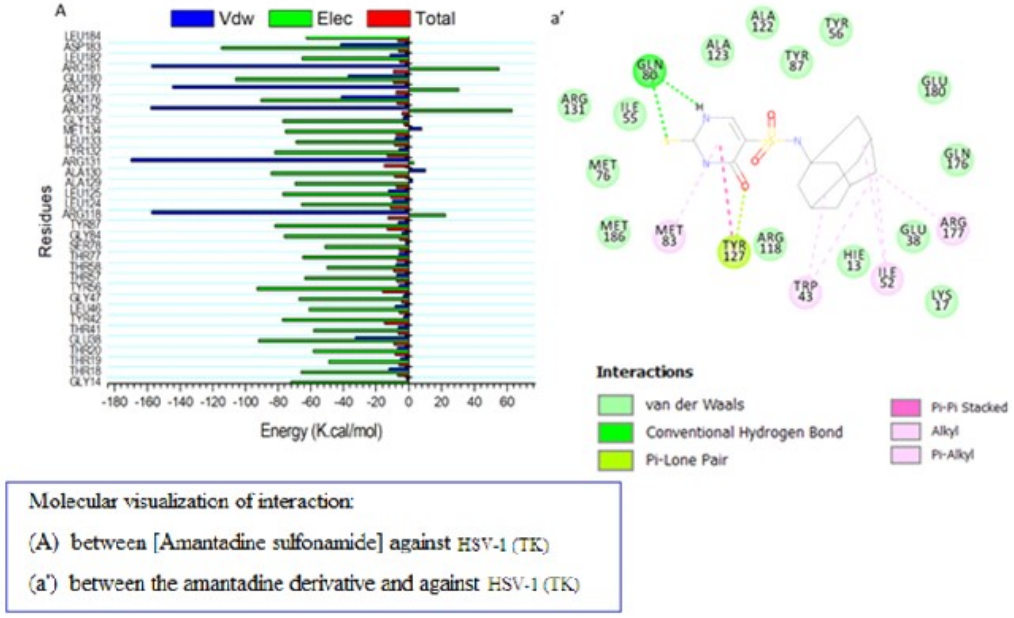

Fig. 5: Molecular visualization

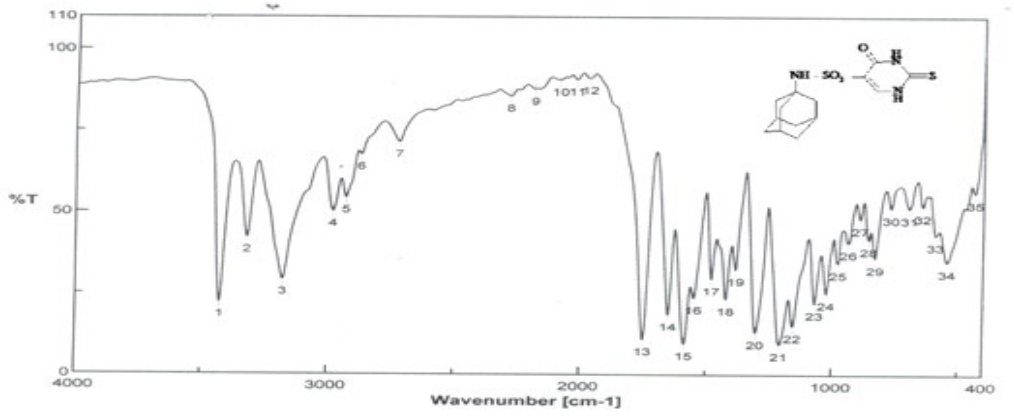

Fig. 6: IR spectrum 5-adamantyl-2-thiopyrimidine sulphonamide.

Table 3: Physiochemical, lipophilicity, water-solubility, pharmacokinetics, drug likeness and medicinal chemistry properties of amantadine sulfonamide derivative.

Physicochemical Properties	
Formula	$C_{14}H_{19}N_3O_3S_2$
Molecular weight	341.45 g/mol
Num. heavy atoms	22
Num. arom. heavy atoms	6
Fraction Csp3	0.71
Num. rotatable bonds	3
Num. H-bond acceptors	4
Num. H-bond donors	3
Molar Refractivity	85.10
TPSA	135.29 Å²
Lipophilicity	
Log Po/w (iLOGP)	1.51
Log Po/w (XLOGP3)	1.48
Log Po/w (WLOGP)	2.76
Log Po/w (MLOGP)	0.87
Log Po/w (SILICOS-IT)	2.78
Consensus Log Po/w	1.88
Water Solubility	
Log S (ESOL)	-2.89
Solubility	4.37e-01 mg/ml ; 1.28e-03 mol/l
Class	Soluble
Log S (Ali)	-3.93
Solubility	4.03e-02 mg/ml ; 1.18e-04 mol/l
Class	Soluble
Log S (SILICOS-IT)	-3.68
Solubility	7.13e-02 mg/ml ; 2.09e-04 mol/l
Class	Soluble
Pharmacokinetics	
GI absorption	High
BBB permeant	No
P-gp substrate	Yes
CYP1A2 inhibitor	No
CYP2C19 inhibitor	Yes
CYP2C9 inhibitor	No
CYP2D6 inhibitor	No
CYP3A4 inhibitor	No
Log Kp (skin permeation)	-7.33 cm/s
Druglikeness	
Lipinski	Yes; 0 violation
Ghose	Yes
Veber	Yes
Egan	No; 1 violation: TPSA>131.6
Muegge	Yes
Bioavailability Score	0.55
Medicinal Chemistry	
PAINS	0 alert
Brenk	1 alert: thiocarbonyl_group
Leadlikeness	Yes
Synthetic accessibility	5.11
Bioactivity and toxicity risk	
Mutagenic	None
Tumorigenic	None
Reproductive effective	High
Irritant	None
GPCR ligand	-0.47
Ion channel modulator	-0.81
Kinase inhibitor	-0.90
Nuclear receptor ligand	-0.86
Protease inhibitor	-0.13
Enzyme inhibitor	-0.43

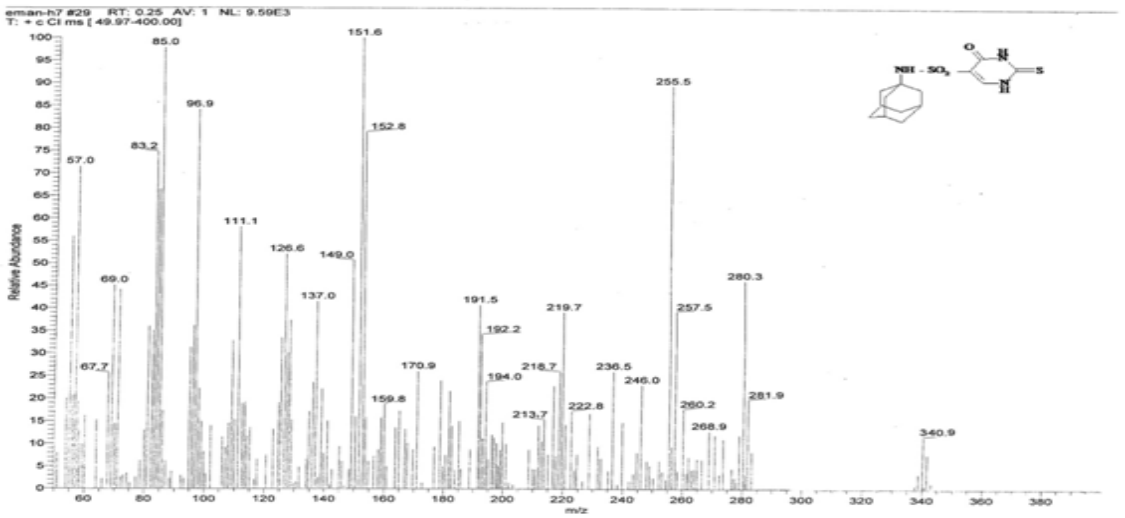

Fig. 7: Mass spectrum 5-adamantyl-2-thiopyrimidine sulphonamide.

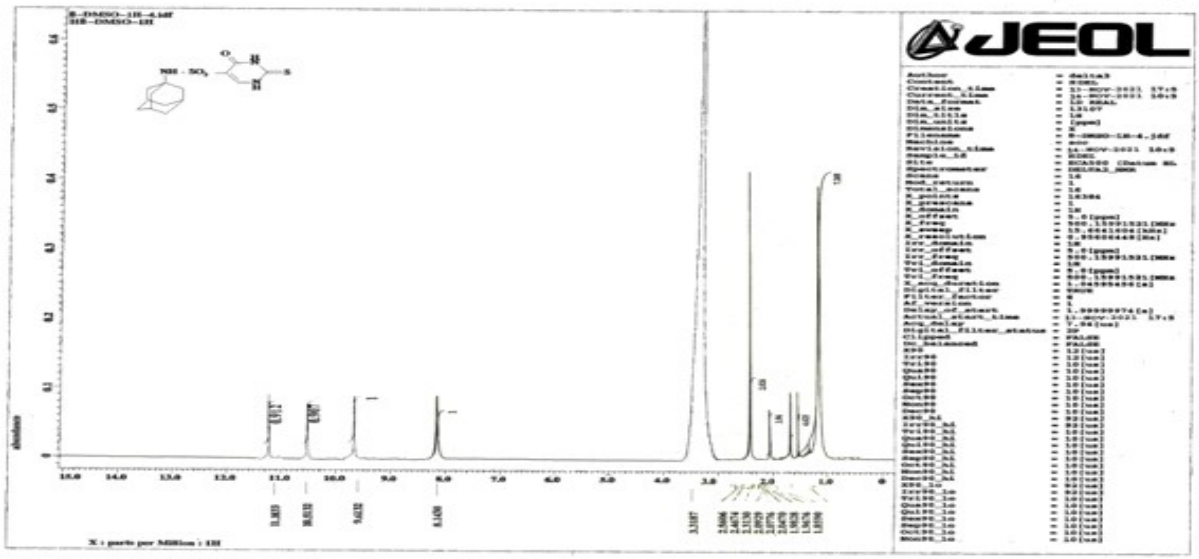

Fig. 8: ^{1}H NMR spectrum 5-adamantyl-2-thiopyrimidine sulphonamide.

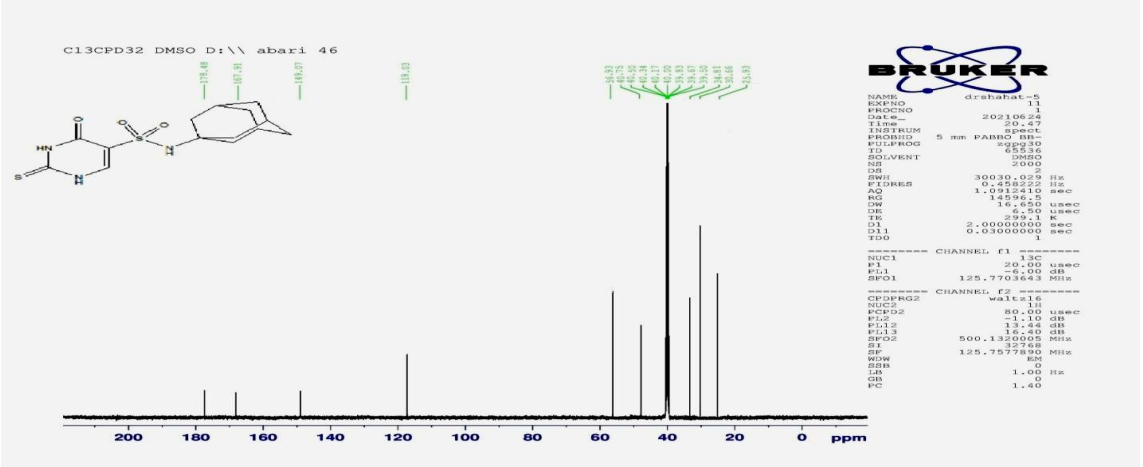

Fig. 9: ^{13}C NMR spectrum 5-adamantyl-2-thiopyrimidine sulphonamide.

Detection of the critical residues accountable for inhibitor binding

The key residues that involved in the attachment of the amantadine derivative and thymidine kinase where shown in fig. 5, the major favourable contribution of the amantadine derivative to HSV-1 (TK) binding is predominantly observed from residues Gly14 (-1.314 kcal/mol), Thr 18 (-11.851 kcal/mol), Thr 19 (-5.05kcal/mol), Thr 20 (-6.78 kcal/mol), Glu 38 (-32.72kcal/mol), Thr 41(-6.517kcal/mol), Thr 42 (-3.06 kcal/mol), Leu 46 (-8.15 kcal/mol), Gly 47 (-3.451 kcal/mol), Tyr 56 (-5.87 kcal/mol), Thr 57 (-7.329 kcal/mol), Thr 57 (-7.68kcal/mol), Thr 77 (-5.84 kcal/mol), Ser 78(-1.736 kcal/mol), Gly 84 (-4.016 kcal/mol),Tyr 87 (-6.343kcal/mol), Arg 118 (-157.14 kcal/mol), Leu 124 (-9.80 kcal/mol), Leu 125 (-12.476 kcal/mol), Arg 131 (-169.73kcal/mol), Tyr 132 (-5.95kcal/mol), Leu 133 (-8.28 kcal/mol), Gly 135 (-3.31 kcal/mol), Arg 175 (-157.74 kcal/mol), Gln 176 (-41.268kcal/mol), Arg 177 (-144.63 kcal/mol), Glu 180(-37.164kcal/mol), Arg 181 (-157.22kcal/mol), Leu 182 (-11.58kcal/mol), Asp 183 (-41.77kcal/mol) and Leu 184(-7.54 kcal/mol) were major contributors (table 3).

ADME prediction

Due to weak ADME qualities, numerous drug molecule candidates stay in phase investigations devoid of a therapeutic molecule. Making some theoretical ADME calculations of newly developed and manufactured drugs can help with highly developed studies in both, living and non-living environments. As a result, few characteristics of the prepared compounds were calculated using Swiss ADME online tools, including: physiochemical properties as well as pharmacokinetics and pharmacodynamic characteristics. Moreover, some properties of the most active amantadine derivative were also listed in Supplementary data as table 3.

The synthesized amantadine sulfonamide derivative has M.Wt. of less than 500 (341.45g/mol). In all lipophilicity estimates, the log P value is >5. It has a moderate to poor solubility in water. Its gastrointestinal absorption was shown to be high and it was also unable to cross the blood-brain barrier. It has no effect on Cyp enzymes, which means it won't interact with other drugs. While drug likeness is high according to Ghose and Egan, it is applicable corresponding to Lipinski, Veber and Muegge's restricted guidelines. Two exceptions to the shortening requirements can be found in the lead likeness property. Other pharmacological chemistry parameters can be used.

DISCUSSION

Chemistry

N-adamantyl amide structure was confirmed with both Elemental assessments and spectral data (Fig 6-9). The IR spectrum revealed absorption ranges at: 3425, 3319, 3178 cm^{-1} due to (3NH`s) and 1749 $cm^{-1}$due to (C=O) group, respectively. The $^{1}$H NMR spectrum showed a multiplet signals in the region at: δ = 1.85-1.09 and 2.31 ppm corresponding to admantyl protons and δ = 8.14, 9.61, 10.51, 11.18ppm corresponding to the pyrimidine CH and NH`s protons. The mass spectrum uncovered a molecular ion peak at m/z 340 (c.f. Instrumental spectral data: IR, Mass, ^{1}HNMR and ^{13}CNMR).

Molecular dynamic and system stability

The findings exposed that amantadine sulfonamide derivative complex system gained a relatively more stable conformation compared to the Apo system. The evaluation of protein structure flexibility upon ligand binding is essential in probing residue behaviour and their association with the ligand during MD simulation. (Heblinga *et al*., 2015; Machaba *et al*., 2018) HSV-1 thymidine kinase residual fluctuations were assessed applying root-mean-square fluctuation (RMSF) algorithm to assess the effect of inhibitor binding towards the corresponding objectives over 50 ns simulations. The computed average RMSF values were 3.77Å and 1.02Å for Apo-TK and amantadine sulfonamide derivative -TK, respectively, (fig. 4B). These data showed that amantadine sulfonamide derivative has the lower residue fluctuation during HSV-1 thymidine kinase inhibition.

ROG was calculated to determine the total compactness of the system in addition to stability upon ligand binding throughout MD simulation (Pan *et al*., 2013; Wijffels *et al*., 2005). The mean Rg data are 19.73Å and 19.64Åfor Apo-TK and amantadine sulfonamide derivative -TK, respectively, (fig. 4C). The observed behavior suggested that compounds amantadine sulfonamide derivative possess a high rigid structure against HSV-1(TK), respectively.

Mechanism of binding interactions based on binding free energy calculation

Drug-ligand binding data provides a valuable means in the structural basis for that ligand's activity. Consequently, calculating protein-ligand binding affinities depending on free binding free energy computations is a crucial method to uncover new protein inhibitors (Cournia *et al*., 2017).

As shown in (table 2), all the reported calculated energy components (except ΔG_{solv}) yielded elevated negative numbers representing good interactions. Binding free energy (ΔG_{bind}) value-40.75 kcal/mol was obtained for the interactions of HSV-1(TK) with the *N*-amantadine derivative.

From the former results we can concluded that: the more +ve Van der Waals energy components drive the amantadine derivative interactions with the HSV-1

thymidine kinase enzyme, leading to the observed binding free energies. Substantial binding free energy values were recorded in gas phase for all the inhibition process with values up to -78.22 kcal/mol. (table 2).

CONCLUSIONS

Allicin and the amantadine sulfonamide derivative showed promising antiherpetic activity; the synergestic effect was studied and was effective. MD studies performed for the amantadine derivative that represents our target compound that has been showed as promising antiherpetic activity by targeting HSV-1 (TK). Agreeing to ADME results, the amantadine derivative agreed to the limiting regulations of Lipinski, Veber and Muegge. Moreover, drug target prediction studies validated the function of amantadine derivative for antiherpetic activity inhibition in addition further studies are required to confirm the synergestic activity of both amantadine derivative and allicin as potent synergistic combination therapy.

REFERENCES

Alen MM, De Burghgraeve T, Kaptein SJ, Balzarini J, Neyts J and Schols D (2011). Broad antiviral activity of carbohydrate-binding agents against the four serotypes of dengue virus in monocyte-derived dendritic cells. *PLoS One*., **6**(6): e21658.

Balgi AD, Wang J, Cheng DY, Ma C, Pfeifer TA and Shimizu Y (2013). Inhibitors of the influenza A virus M2 proton channel discovered using a high-throughput yeast growth restoration assay. *PLOS ONE.*, **8**(2): e55271.

Bright RA, Medina MJ, Xu X, Perez-Oronoz G, Wallis TR, Davis XM, Povinelli L, Cox NJ and Klimov AI (2000).Incidence of adamantane resistance among influenza A (H3N2) viruses isolated worldwide from 1994 to 2005: A cause for concern. *Lancet*., **366**(9492): 1175-1181.

Champness JN, Bennett MS, Wien F, VisseR, Summers WC, Herdewijn P, De Clercq E, Ostrowski T, Jarvest RL and Sanderson MRJPS (1998). Exploring the active site of herpes simplex virus type-1 thymidine kinase by X-ray crystallography of complexes with aciclovir and other ligands. *Proteins: Struct. Funct. Genet.*, **32**(3): 350-361.

Cournia Z, Allen B and Sherman W (2017). Relative binding free energy calculations in drug discovery: recent advances and practical considerations. *J. Chem. Inf. Model.*, **57**(12): 2911-2937.

Drissi M, Benhalima N, Megrouss Y, Rachida R, Chouaih A and Hamzaoui F (2015). Theoretical and experimental electrostatic potential around the m-nitrophenol molecule. *Molecules*. **20**(3): 4042-54.

Genheden S and Ryde U (2015). The MM/PBSA and MM/GBSA methods to estimate ligand-binding affinities. *Expert. Opin. Drug. Discov.*, **10**(5): 449-461.

Hadi Gh, Ahmad T, Abdolvahab M, Alijan T, Farah B, Masoumeh Z, Mohammad F, Davod J, Seyed JK, Maryam E, Vahid PM, Angila AP and Seyed HM (2019). Inhibition of H_1N_1 influenza virus infection by zinc oxide nanoparticles: another emerging application of nanomedicine. *J. Biomed. Sci.*, **26**(70): 1-10.

Harazem R, Rahman SE and El-Kenawy AA (2019). Evaluation of antiviral activity of allium cepa and allium sativum extracts against newcastle disease virus. *Alex. J. Vet. Sci.*, **61**(1): 108-118.

Hayes JM and Archontis G (2012). MM-GB(PB)SA calculations of protein-ligand binding free energies. molecular dynamics-studies of synthetic biological macromolecules. *In. Tech. Ch*., **9**: 171-190.

Heblinga J, Bianchia L, Bassoa FG, Scheffela DL, Soaresa DG, Carrilhob MRO, Pashleyc DH,Tjäderhaned L and de Souza Costa CA (2015). Cytotoxicity of dimethyl sulfoxide (DMSO) in direct contact with odontoblast-like cells. *Dent. Mater*., **31** (4): 399-405.

Holsinger DI, Nichani D, Pinto LH and Lamb RA (1994). Influenza A virus M2 ion channel protein: A structure-function analysis. *J. Virol*., **68**(3): 1551-1563.

Hospital A, Goñi JR, Orozco M and Gelpí JL (2015). Molecular dynamics simulations: advances and applications. *Adv. Appl. Bioinform. Chem*., **8**: 37-47.

Hou T, Wang J, Li Y and Wang W (2010). Assessing the performance of the MM/PBSA and MM/GBSA methods. 1. The accuracy of binding free energy calculations based on molecular dynamics simulations. *J. Chem. Inf. Model.,* **51**(1): 69-82.

Hubsher GH, Haider M and Okum M (2012). Amantadine: the journey from fighting flu to treating parkinson disease. *Neurology*., **78**(14): 1096-1099.

Kollman PA, Massova I, Reyes C, Kuhn B, HuoS, Chong L, Lee M, Lee T, Duan Y and Wang W (2000). Calculating structures and free energies of complex molecules: combining molecular mechanics and continuum models. *Acc. Chem. Res*., **33**(12): 889-897.

Lee TS, Cerutti DS, MermelsteinD, Lin C, LeGrand S, GieseTJ, Roitberg A, Case DA and Walker RC (2018). GPU-Accelerated molecular dynamics and free energy methods in amber18: performance enhancements and new feature. *J. Chem. Inf. Model.*, **58**(10): 2043-2050.

Li H, Robertson AD and Jensen JHJPS (2005). Very fast empirical prediction and rationalization of protein pKa values. *Proteins: Struct. Funct. Genet.*, **61**(4): 704-721.

Liu X, Ouyang S, Yu B, Liu Y, Huang K, Gong J, Zheng S, Li Z, Li H and Jiang H (2010). Proteome-wide prediction of protein-protein interactions from high-throughput data. *Nucleic Acids Res*., **38**(2): 609-614.

Machaba KE, Mhlongo NN and Soliman ME (2018). Induced mutation proves a potential target for TB therapy: A molecular dynamics study on LprG. *Cell Biochem. Biophys*., **76**(3): 345-356.

Pan L and Patterson JC (2013). Molecular dynamics study of Zn(Aβ) and $Zn(A\beta)_2$. *PLoS One*., **8**(9): e70681.

Pettersen EF, Goddard TD, Huang CC, Couch GS, Greenblatt DM and Meng EC (2004). UCSF chimera-A visualization system for exploratory research and analysis. *J. Comput. Chem*., **25**(13): 1605-1612.

PTRAJ and CPPTRAJ. PTRAJ and CPPTRAJ: software for processing and analysis of molecular dynamics trajectory data. *J. Chem. Theory comput.*, **9**(7): 3084-3095.

Rahman S, Salehin F and Iqbal A (2011). In vitro antioxidant and anticancer activity of young Zingiber officinale against human breast carcinoma cell lines. *Complement. Altern. Med*., **11**(76):1-7.

Ranitha M, Nurlidia M, Muhammad RS, Yoshimitsu U and Zahid M (2017). Optimisation of ultrasonic-assisted extraction (UAE) of allicin from garlic (Allium sativum L.). *Chem. Eng. Trans*., **56**: 1747-1752.

Roe DR, Cheatham III TE, PTRAJ and CPPTRAJ (2013). Seifert E (2014). OriginPro 9.1: scientific data analysis and graphing software-software review. *J. Chem. Inf. Model.*, **54**(5): 1552-1552.

Saif MH, Ashwaq NA, Yasmeen AH, Samir MA and Najah R Hadi (2020). The potential antiviral activity of a novel pyrimidine derivative against herpes simplex virus type-1 (HSV-1). *Sys. Rev. Pharm*., **11**(2): 795-806.

Samir MA, Shima MA, Yara EM and Samar SF (2021). Synthesis and evaluation of some uracil nucleosides as promising anti-Herpes simplex virus 1 agents. *Molecules*., **26** (10):2988.

Vioreca MC, Irina G, Ioana CM, Elisabela IG, Maria IM, Ortansa C and Mariana CC (2021). Demonstration of allium sativum extract inhibitory effect on biodeteriogenic microbial strain growth, biofilm development, and enzymatic and organic acid production. *Molecules*., **26**(23): 7195.

Yoshiteru K, Mamoru N and Yumiko I (2006). Frequency of amantadine-resistant influenza a virus isolated from 2001 - 02 to 2004 - 05 in nara prefecture. *Jpn. J. Infect*., **59**: 197-199.

Wang J, Wang W, Kollman PA and Case DA (2006). Automatic atom type and bond type perception in molecular mechanical calculations. *J. Mol. Graph. Model*., **25**(2): 247-260.

Wijffels G, Dalrymple B, Kongsuwan K and Dixon NE (2005). Critical review conservation of eubacterial replicases. *IUBMB life*., **57**(6): 413-419.

Zandi K, Taherzadeh M, Yaghoubi R, Tajbakhsh S, Rastian Z and Sartavi K (2009). Antiviral activity of avicennia marina against herpes simplex virus type 1 and vaccine strain of poliovirus (An in vitro study). *J. Med. Plant. Res.,* **3** (10): 771-775.